

MERGER HISTORIES OF GALAXY HALOS AND IMPLICATIONS FOR DISK SURVIVAL

KYLE R. STEWART¹, JAMES S. BULLOCK¹, RISA H. WECHSLER², ARIYEH H. MALLER³, AND ANDREW R. ZENTNER⁴

ABSTRACT

We study the merger histories of galaxy dark matter halos using a high resolution Λ CDM N -body simulation. Our merger trees follow $\sim 17,000$ halos with masses $M_0 = (10^{11} - 10^{13})h^{-1}M_\odot$ at $z = 0$ and track accretion events involving objects as small as $m \simeq 10^{10}h^{-1}M_\odot$. We find that mass assembly is remarkably self-similar in m/M_0 , and dominated by mergers that are $\sim 10\%$ of the final halo mass. While very large mergers, $m \gtrsim 0.4M_0$, are quite rare, sizeable accretion events, $m \sim 0.1M_0$, are common. Over the last ~ 10 Gyr, an overwhelming majority ($\sim 95\%$) of Milky Way-sized halos with $M_0 = 10^{12}h^{-1}M_\odot$ have accreted at least one object with greater total mass than the Milky Way disk ($m > 5 \times 10^{10}h^{-1}M_\odot$), and approximately 70% have accreted an object with more than twice that mass ($m > 10^{11}h^{-1}M_\odot$). Our results raise serious concerns about the survival of thin-disk dominated galaxies within the current paradigm for galaxy formation in a Λ CDM universe. In order to achieve a $\sim 70\%$ disk-dominated fraction in Milky Way-sized Λ CDM halos, mergers involving $m \simeq 2 \times 10^{11}h^{-1}M_\odot$ objects must not destroy disks. Considering that most thick disks and bulges contain old stellar populations, the situation is even more restrictive: these mergers must not heat disks or drive gas into their centers to create young bulges.

Subject headings: cosmology: theory — dark matter — galaxies: formation — galaxies: halos — methods: N -body simulations

1. INTRODUCTION

In the cold dark matter (CDM) model of structure formation, dark matter halos form via the continuous accretion of smaller systems (Peebles 1982; Blumenthal et al. 1984; Davis et al. 1985; Fakhouri & Ma 2007; Neistein & Dekel 2008; Cole et al. 2008). Mergers of the type predicted can help explain many properties of the observed universe. Major mergers are believed to play an important role in shaping the Hubble sequence (Toomre & Toomre 1972; Barnes 1988; Hernquist 1993; Naab & Burkert 2003; Khochfar & Burkert 2005; Cox et al. 2006a; Robertson et al. 2006a,b,c; Maller et al. 2006; Jesseit et al. 2007; Bournaud et al. 2007) and triggering star formation and AGN activity (Mihos & Hernquist 1996; Kolatt et al. 1999; Cox et al. 2006b; Woods et al. 2006; Barton et al. 2007). Minor mergers may help explain the origin of thick disks (Quinn et al. 1993; Walker et al. 1996; Abadi et al. 2003; Brook et al. 2004; Dalcanton et al. 2005; Kazantzidis et al. 2007; Hayashi & Chiba 2006), cause anti-truncation (Younger et al. 2007), and produce extended diffuse light components around galaxies (Johnston et al. 1996; Helmi & White 1999; Bullock et al. 2001; Bullock & Johnston 2005; Purcell et al. 2007; Bell et al. 2007). However, there is lingering concern that mergers are too common in CDM cosmologies for thin disk-dominated systems to survive (Toth & Ostriker 1992; Wyse 2001; Kormendy & Fisher 2005; Kautsch et al. 2006). In this paper we present the merger statistics necessary for addressing this issue.

The formation of disk galaxies within hydrody-

namic simulations in hierarchical CDM cosmologies has proven problematic (e.g. Navarro & Steinmetz 2000). While there have been some successes in forming galaxies with disks in cosmological simulations (Abadi et al. 2003; Sommer-Larsen et al. 2003; Brook et al. 2004; Robertson et al. 2004; Kaufmann et al. 2007a; Governato et al. 2007), the general problem is far from resolved. The resultant disks are often fairly thick and accompanied by large bulges, and the systems that form disks tend to have special merger histories. The resultant thick disk and bulge stars also tend towards a broad range of stellar ages, instead of being dominated by predominantly old stars. Moreover, the successes depend strongly on effective models that describe physics on scales far below the simulation resolution, which are poorly understood. Given the current difficulties in understanding *ab initio* disk formation, one can consider a less ambitious, but more well-posed question. Even if disk galaxies can form within CDM halos, can they survive the predicted merger histories?

Unfortunately, the prevalence of thin-disk or even disk-dominated galaxies in the universe is difficult to quantify with large observational samples. Some promising approaches use asymmetry vs. concentration to define morphological type (e.g., Ilbert et al. 2006), and some use a combination color and concentration indicators (e.g. Choi et al. 2007; Park et al. 2007). Despite the wide range of definitions, the general consensus in the literature is that $\sim 70\%$ of $\sim 10^{12}h^{-1}M_\odot$ halos host disk-dominated, late-type galaxies (e.g. Weinmann et al. 2006; van den Bosch et al. 2007; Ilbert et al. 2006; Choi et al. 2007; Park et al. 2007). We adopt this number for the sake of discussion in what follows, but none of our primary results on merger statistics depend on this number.

Also relevant to the discussion of galaxy merger histories is the prevalence of pure disk galaxies in the universe. Kautsch et al. (2006) have compiled a statistically meaningful sample of edge-on disk galaxies and found

¹ Center for Cosmology, Department of Physics and Astronomy, The University of California at Irvine, Irvine, CA, 92697, USA

² Kavli Institute for Particle Astrophysics & Cosmology, Physics Department, and Stanford Linear Accelerator Center, Stanford University, Stanford, CA 94305, USA

³ Department of Physics, New York City College of Technology, 300 Jay St., Brooklyn, NY 11201, USA

⁴ Department of Physics and Astronomy, University of Pittsburgh, Pittsburgh, PA 15260, USA

that $\sim 16\%$ of these objects are “simple disks” with no observable bulge component. In principle, this statistic places strong constraints on the merger histories of galaxies. Moreover, a large fraction of disk galaxies with bulges contain pseudo-bulges, which may be the products of secular processes and not the remnants of an early merger event (e.g. Kormendy & Kennicutt 2004; Carollo et al. 2007). These cases provide further motivation to quantify the predicted merger histories of galaxy halos in the favored CDM cosmology.

Here we use a large dissipationless cosmological Λ CDM N -body simulation to track the merger histories of an ensemble of $\sim 17,000$ halos with $z = 0$ masses $M_0 = 10^{11} - 10^{13} h^{-1} M_\odot$. We focus on halos of fixed mass at $z = 0$, and concentrate specifically on Milky Way-sized systems, $M_0 \simeq 10^{12} h^{-1} M_\odot$. We categorize the accretion of objects as small as $m \simeq 10^{10} h^{-1} M_\odot$ and focus on the infall statistics into *main progenitors* of $z = 0$ halos as a function of lookback time. As discussed below, the *main progenitor* is defined to be the most massive progenitor of a $z = 0$ halo tracked continuously back in time.

A *merger* is defined here to occur when an infalling halo first crosses within the virial radius of the main progenitor. In most cases we do not track subhalo evolution after accretion. We have chosen to track mergers in this way in order to provide a robust prediction. An understanding of an accreted halo’s subsequent orbital evolution and impact with the central disk region is essential for any complete understanding of *galaxy* merger statistics. However, this evolution will be sensitive to the baryonic distribution within both the main progenitor halo and the satellites themselves. The *halo* merger rate we present is a relatively clean measure that can be used as a starting point for more detailed investigations of galaxy–galaxy encounters. Still, it is worth pointing out that for most of the mergers we consider, impacts with the central disk region should occur relatively shortly after accretion. As we show in the Appendix, events with $m \gtrsim 0.1 M_0$ typically happen at a redshift z when the main progenitor mass, M_z , is significantly smaller than M_0 , such that the merger ratio is fairly large $m/M_z \gtrsim 0.2$. Therefore, even ignoring the enhanced orbital decay that will be caused by a central disk potential, the dynamical friction decay times are expected to be short for these events, with central impacts occurring within $\tau \lesssim 3$ Gyr for typical orbital parameters (Boylan-Kolchin et al. 2007; Zentner et al. 2005; Zentner & Bullock 2003). As discussed in conjunction with Figure 5 in §3, destruction times of ~ 3 Gyr are consistent with our measurements of subhalo evolution.

The outline of this paper is as follows. In §2 we discuss the numerical simulations used and the method of merger tree construction. In §3 we present our principle results, which characterize the accretion mass functions of halos and the fraction of halos with mergers as a function of lookback time. In §4 we discuss these results in reference to the problem of disk survival in a hierarchical universe, and we summarize our main conclusions in §5.

2. SIMULATIONS

Our simulation consists of 512^3 particles, each with mass $m_p = 3.16 \times 10^8 h^{-1} M_\odot$, evolved within a comoving cubic volume of $80 h^{-1}$ Mpc on a side using the Adaptive Refinement Tree (ART) N -body code (Kravtsov et al.

1997, 2004). The cosmology is a flat Λ CDM model, with parameters $\Omega_M = 1 - \Omega_\Lambda = 0.3$, $h = 0.7$, and $\sigma_8 = 0.9$. The simulation root computational grid consists of 512^3 cells, which are adaptively refined to a maximum of eight levels, resulting in a peak spatial resolution of $1.2 h^{-1}$ kpc, in comoving units. This simulation and the methods we use to construct merger trees have been discussed elsewhere (Allgood et al. 2006; Wechsler et al. 2006). Here we give a brief overview and refer the reader to those papers for a more complete discussion.

Field dark matter halos and subhalos are identified using a variant of the bound density maxima algorithm (Klypin et al. 1999). A *subhalo* is defined as a dark matter halo whose center is positioned within the virial radius of another, more massive halo. Conversely, we define a *field halo* to be a dark matter halo that does not lie within the virial radius of a larger halo. The virial radius is defined as the radius of a collapsed self-gravitating dark matter halo within which the average density is Δ_{vir} times the mean density of the universe. For the family of flat cosmologies ($\Omega_m + \Omega_\Lambda = 1$) the value of Δ_{vir} can be approximated by (Bryan & Norman 1998):

$$\Delta_{vir} = \frac{18\pi^2 + 82(\Omega_m(z) - 1) - 39(\Omega_m(z) - 1)^2}{\Omega_m(z)}. \quad (1)$$

Masses, M , are defined for field halos as the mass enclosed within the virial radius, so that $M = (4\pi/3)R^3\Omega_m\rho_c\Delta_{vir}$. With these definitions, the virial radius for halos of mass M at $z = 0$ is given by:

$$R \simeq 205 h^{-1} \text{kpc} \left(\frac{M}{10^{12} h^{-1} M_\odot} \right)^{1/3}. \quad (2)$$

Note that this mass definition based on a fixed overdensity is largely conventional, and is traditionally used as a rough approximation for the radius within which the halos are virialized. We refer the reader to the recent work of Cuesta et al. (2007) for further discussion of this issue.

Halo masses become more difficult to define in crowded environments. For example, if two halos are located within two virial radii of each other, mass double-counting can become a problem. Also, subhalos can become tidally stripped if they are accreted into a larger halo. While the stripped material typically remains bound to the larger host halo, it is no longer bound to the smaller subhalo and should not be included in the subhalo’s mass. In these cases, the standard virial overdensity definitions are not appropriate. In order to overcome this ambiguity, we always define a halo’s radius and mass as the minimum of the virial mass and a “truncation mass” – defined as the mass within the radius where the log-slope of the halo density profile becomes flatter than -0.5 . This definition of truncation mass is a relatively standard practice when dealing with simulations of this kind (e.g. Klypin & Holtzman 1997; Kravtsov et al. 2004; Zentner et al. 2005), and we follow this convention to remain consistent with other work in this field. In practice, our field halos have masses and radii defined by the standard virial relations ($\sim 98\%$ of all non-subhalos). It is fair then to interpret our merger rates as infall rates into halo virial radii. The masses of objects just prior to infall are more likely affected by this definition, but the overall effect on our results is not large. As a test, we

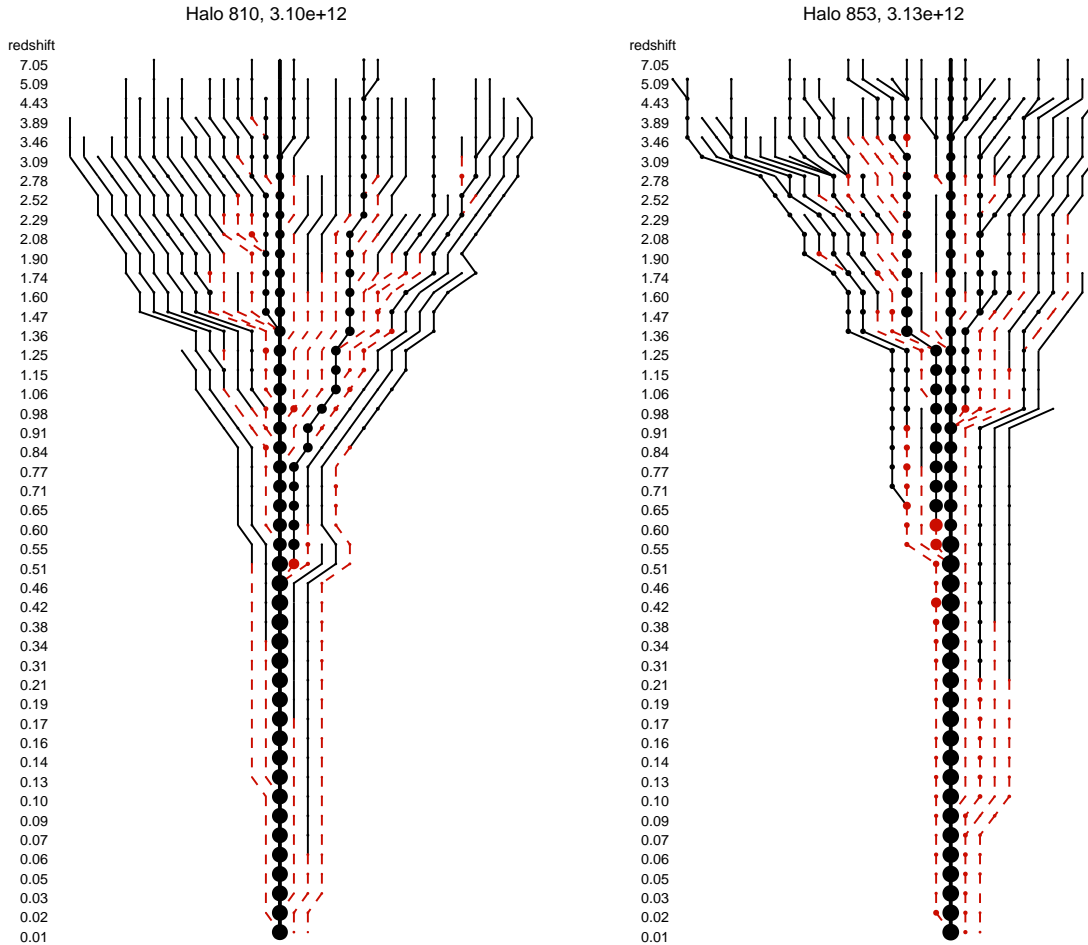


FIG. 1.— Sample merger trees, for halos with $M_0 \simeq 10^{12.5} h^{-1} M_\odot$. Time progresses downward, with the redshift z printed on the left hand side. The bold, vertical line at the center corresponds to the main progenitor, with filled circles proportional to the radius of each halo. The minimum mass halo shown in this diagram has $m = 10^{9.9} h^{-1} M_\odot$. Solid (black) and dashed (red) lines and circles correspond to isolated field halos, or subhalos, respectively. The dashed (red) lines that do not merge with main progenitor represent surviving subhalos at $z = 0$. *Left*: A “typical” merger history, with a merger of mass $m \simeq 0.1M_0 \simeq 0.5M_z$ at $z = 0.51$. *Right*: A halo that experiences an unusually large merger $m \simeq 0.4M_0 \simeq 1.0M_z$ at $z = 0.65$.

have redone our main analysis using an (extrapolated) virial mass for infalling halos. The results on fractional merger rates change only at the $\sim 5\%$ level.

In the event that a halo experiences a close pass with another halo—entering within the virial radius for a short time, then exiting the virial radius never to return—the two halos are considered isolated, even though one may lie within the virial radius of the other. Conversely, if the smaller halo falls back within the virial radius and the two halos subsequently merge together, then we continue to consider the smaller halo a subhalo even during the time when it lies outside the virial radius of its host. This has been referred to as the “stitching” method—as opposed to “snipping,” which would count the above example as two separate mergers (Fakhouri & Ma 2007).

By constructing mass functions, we find that these halo catalogs are complete to a minimum mass $10^{10} h^{-1} M_\odot$. This allows us to measure the accretion of objects 10 times smaller than $10^{11} h^{-1} M_\odot$ halos, or objects up to 1000 times smaller than $10^{13} h^{-1} M_\odot$ halos. In all cases, we denote the mass of an accreted object as m . Overall we have a total of 17,241 halos in our sample with

$M_0 > 10^{11} h^{-1} M_\odot$, and (6642, 2479, 911, and 298) halos in logarithmically-spaced mass bins centered on $\log M_0 = (11.5, 12.0, 12.5, \text{ and } 13.0)$ respectively, in units of $h^{-1} M_\odot$.

Our merger tree construction mirrors that described in Kravtsov et al. (2004) and uses 48 stored timesteps that are approximately equally spaced in expansion factor between the current epoch $a = (1+z)^{-1} = 1.0$ and $a = 0.0443$. We use standard terminologies for *progenitors* and *descendant*. Any halo at any timestep may have any number of *progenitors*, but a halo may have only one *descendant*—defined to be the single halo in the next timestep that contains the majority of this halo’s mass. We use the terms “merger” and “accretion” interchangeably to designate the infall of a smaller halo into the virial radius of a larger one. The term *main progenitor* is used to reference the most massive progenitor of a $z = 0$ halo tracked continuously back in time.

Throughout most of this work we present results in terms of absolute mass thresholds on the infalling mass m . Our principle statistics are quantified using the infalling mass thresholds in terms of the final $z = 0$ mass

of the main progenitor halo (e.g. $m > 0.1M_0$). Indeed, many of our results are approximately self-similar with respect to halo mass when the infalling mass cut is defined in this scaled manner. By definition, the maximum mass that a merging halo can have is $m = 0.5M_0$. Note that it is common in the literature to study the *merger ratio* of an infalling object, m/M_z , where M_z is the main progenitor mass at the redshift z , just prior to the merger. Here, M_z *does not* incorporate the mass m itself and therefore m/M_z has a maximum value of 1.0. A parallel discussion that uses m/M_z is presented in the Appendix, but the absolute mass thresholds are used as our primary means to quantify merger statistics in the main part of this paper. We make this choice for two reasons. First, it is relatively easy to understand completeness effects using a fixed threshold in m , while completeness in m/M_z will vary as a function of time and will change from halo to halo depending on its particular mass accretion history. Second, an event with $m/M_z \sim 1$ does not necessarily imply that the infalling object m is large compared to the final halo mass M_0 . In order to be conservative, we would like to restrict ourselves to mergers that are large in an absolute sense compared to typical galaxy masses today.

Figure 1 shows two pictorial examples of merger trees for halos with approximately equal $z = 0$ masses $M_0 \simeq 10^{12.5}h^{-1}M_\odot$. Time runs from top to bottom and the corresponding redshift for each timestep is shown to the left of each tree. The radii of the circles are proportional to the halo radius $R \sim M^{1/3}$, while the lines show the descendent–progenitor relationship. The color and type of the connecting lines indicate whether the progenitor halo is a field halo (solid black) or a subhalo (dashed red). The most massive progenitor at each timestep — the main progenitor — is plotted in bold down the middle. The ordering of progenitor halos in the horizontal direction is arbitrary. Once a halo falls within the radius of another halo, it becomes a subhalo and its line-type changes from black solid to red dashed. When subhalo lines connect to a black line this corresponds to a central subhalo merger or to a case when the subhalo has been stripped to the point where it is no longer identified. When field halos connect directly to a progenitor without becoming subhalos in the tree diagram it means that the subhalo is stripped or merged within the timestep resolution of the simulation. Halos that are identified as subhalos of the main halo at $z = 0$ are represented by the dashed-red lines that reach the bottom of the diagram without connecting to the main progenitor line.

Note that the extent to which we can track a halo after it has become a subhalo, and the point at which a subhalo is considered “destroyed” is dependent both on spacing of our output epochs and mass resolution of the simulation. This is another reason why we count mergers when a halo falls within the virial radius (when the lines in Figure 1 change from solid-black to dashed-red) and not when a subhalo experiences a central merger with its host.

The left diagram (“halo 810”) in Figure 1 shows a fairly typical merger history, with a merger of mass $m \simeq 0.1M_0$ at $z \simeq 0.51$. The merger ratio at the time of the merger was $m/M_z \simeq 0.5$. The right diagram (“halo 853”) shows a very rare type of merger history with a massive event

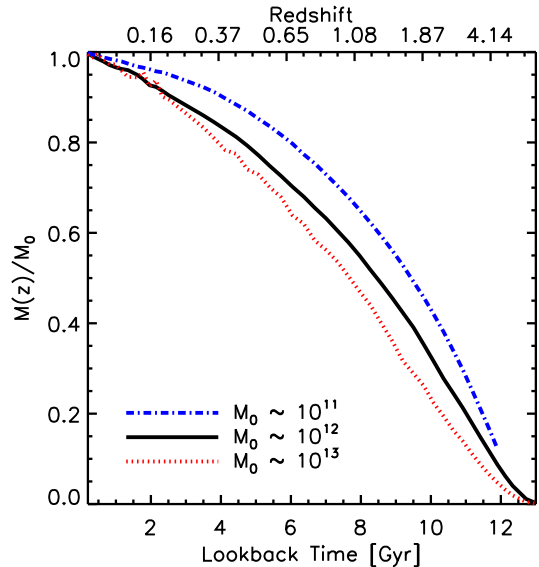


FIG. 2.— Average mass accretion histories for three bins in halo mass, as a function of lookback time. Each bin gives the average for bins of size $\log M_0 = 0.5$, centered on the stated value. More massive halos accreted a larger fraction of their mass at late times.

$m \simeq 0.4M_0$ at $z \simeq 0.65$. This was a nearly equal-mass accretion event at the time of the merger, $m/M_z \simeq 1.0$. Note that neither of these large mergers survive for long as resolved subhalos — they quickly lose mass and merge with the central halo. Each of these halos has two $\sim 10^{10}h^{-1}M_\odot$ subhalos that survive at $z = 0$.

3. RESULTS

3.1. Accretion Histories and Mass Functions

The literature is rich with work on the cumulative mass accretion histories of halos as a function of redshift (e.g. Wechsler et al. 2002; Zhao et al. 2003; Tasitsiomi et al. 2004; Li et al. 2007, and references therein). We begin by re-examining this topic for the sake of completeness. Figure 2 shows average main progenitor mass accretion histories, $M_z = M(z)$, for halos of three characteristic final masses, $M_0 = M(z = 0)$. We confirm previous results that halo mass accretion histories are characterized by an initial rapid accretion phase followed by a slower accretion phase, and that more massive halos experience the rapid accretion phase later than less massive halos (Wechsler et al. 2002). Milky Way-sized halos with $M_0 = 10^{12}h^{-1}M_\odot$ will, on average, accrete half of their mass by $z \simeq 1.3$, corresponding to a lookback time of ~ 8.6 Gyr.

While Figure 2 provides some insight into *when* mass is accreted into halos, we are also interested in characterizing *how* this mass is accreted. (Ultimately, we will present merger statistics for a joint distribution of both time *and* mass ratio.) Now we investigate the mass function $n(m)$ of objects larger than m that have merged into the main progenitor over its history. The solid line in Figure 3 shows $n(m)$ averaged over halos in the $M_0 = 10^{12}h^{-1}M_\odot$ bin, plotted as a function of m/M_0 . On average, Milky Way-sized halos with $M_0 \simeq 10^{12}h^{-1}M_\odot$ experience ~ 1 merger with objects larger than $m \sim 10^{11}h^{-1}M_\odot$, and ~ 7 mergers with objects larger than $m \sim 10^{10}h^{-1}M_\odot$ over the course of their

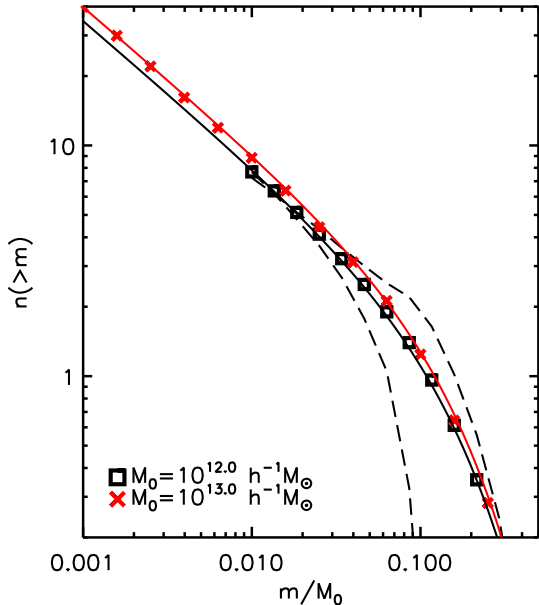


FIG. 3.— Mass functions of accreted material, with respect to the final halo mass. Lines show the cumulative number of mergers that a halo experiences with objects larger than m/M_0 , integrated over the main progenitor’s formation history. The (black) squares show the average for $10^{12}h^{-1}M_\odot$ halos; (red) crosses show the average for $10^{13}h^{-1}M_\odot$ halos. Lines through the data points show the fits given by Equation 3. The upper/lower dashed lines indicate the $\sim 25\%/20\%$ of halos in the $10^{12}h^{-1}M_\odot$ sample that have experienced exactly two/zero $m \geq 0.1M_0$ merger events. Approximately 45% of halos have exactly one $m \geq 0.1M_0$ merger event; these systems have mass accretion functions that resemble very closely the average.

lives.

For some purposes, an analytic characterization of the accreted mass function will be useful. We have investigated the average $n(m)$ function for halos in the mass range $M_0 = 10^{11.5} - 10^{13}h^{-1}M_\odot$ and find that the shape of this function is remarkably similar over this range (smaller M_0 were neglected in order to achieve a reasonable range in m/M_0). Specifically, we find that $n(m)$ is well-characterized by a simple function of $x \equiv m/M_0$:

$$n(>x) = Ax^{-\alpha}(0.5-x)^\beta, \quad (3)$$

with $\beta = 2.3$, $\alpha = 0.61$, and $x \leq 0.5$ by construction. Interestingly, we find that the overall normalization increases monotonically with halo mass, and that the trend can be approximated as $A(M_0) \simeq 0.47 \log_{10}(M_0) - 3.2$, where M_0 is in units of $h^{-1}M_\odot$. This mass-dependent normalization, together with Equation 3, reproduces our measured $n(m)$ functions quite well — to better than 5% at all m in smaller halos ($M_0 = 10^{11.5} - 10^{12}h^{-1}M_\odot$), and (somewhat worse) to 15% at higher masses ($M_0 = 10^{12.5} - 10^{13}h^{-1}M_\odot$).⁵

We would also like to understand the scatter in the accreted mass function from halo to halo at fixed M_0 . It is not appropriate to simply describe the variation in $n(m)$ at a fixed mass, because the total mass accreted is constrained to integrate to less than M_0 . This means that the number of small objects accreted may be anti-correlated with the number of large objects accreted.

⁵ The quoted errors are restricted to $n > 0.05$.

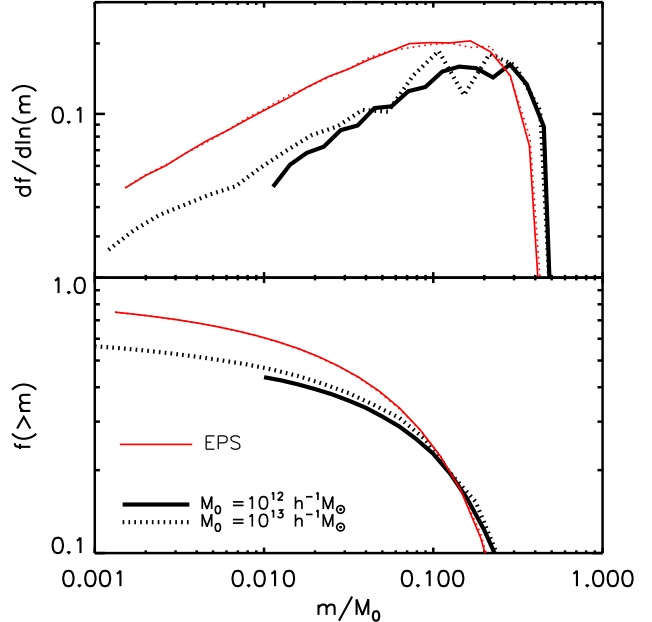


FIG. 4.— The fraction of halo’s final mass M_0 accreted from objects of mass m/M_0 , integrated over time. The differential (upper) and cumulative (lower) mass fractions are shown. The thick (black) lines show simulation results and the thin (red) lines show the prediction from standard Extended Press Schechter (EPS). Accretions with $m \simeq (0.03 - 0.3)M_0$ dominate the mass buildup in halos of all M_0 . The distributions are approximately self-similar with host halo mass. This is in reasonably good agreement with the EPS expectation, although the EPS fractions systematically sit above the simulation results.

With this in mind, we provide an illustration of the scatter with the two dashed lines in Figure 3. The upper dashed line shows the average $n(m)$ for the $\sim 25\%$ of halos that have experienced exactly two accretion events larger than $m = 0.1M_0$. The lower dashed line shows the average $n(m)$ for the $\sim 20\%$ of halos that have experienced exactly zero $m > 0.1M_0$ accretion events. Approximately $\sim 45\%$ of halos have exactly one $m > 0.1M_0$ event, and these have an average accreted mass function that is very similar to the overall average shown by solid (black) line in Figure 3. Halos with fewer large mergers show a slight tendency to have more small mergers, but the effect is not large.

Figure 4 presents some of the same information shown in Figure 3, but now in terms of the mass fraction, $f(m)$, accreted in objects larger than m for $M_0 = 10^{12}$ and $10^{13}h^{-1}M_\odot$ halos (thick lines, see legend). The upper panel in Figure 3 shows the differential fraction, $df/d\ln m = (-m^2/M_0)dn/dm$, while the lower panel plots the integrated fraction $f(m)$. As before, we have normalized the accreted masses, m , by the final $z = 0$ main progenitor mass M_0 . We find that $f(>m)$ is also well fit by Equation 3 (to better than 10% across all masses $M_0 = 10^{12} - 10^{14}h^{-1}M_\odot$)⁶. As before, $x \equiv m/M_0$, but now $A(M_0) \simeq 0.17 \log_{10}(M_0) - 0.36$, with M_0 still in units of $h^{-1}M_\odot$. The best fit parameters are $\alpha = 0.05$, and $\beta = 2.3$. The lines are truncated at $m/M_0 = 0.01$ and 0.001 , corresponding to our fixed resolution limit at $m = 10^{10}h^{-1}M_\odot$. The thin (red) lines of the same line types show the same quan-

⁶ The quoted errors are restricted to $f > 0.1$.

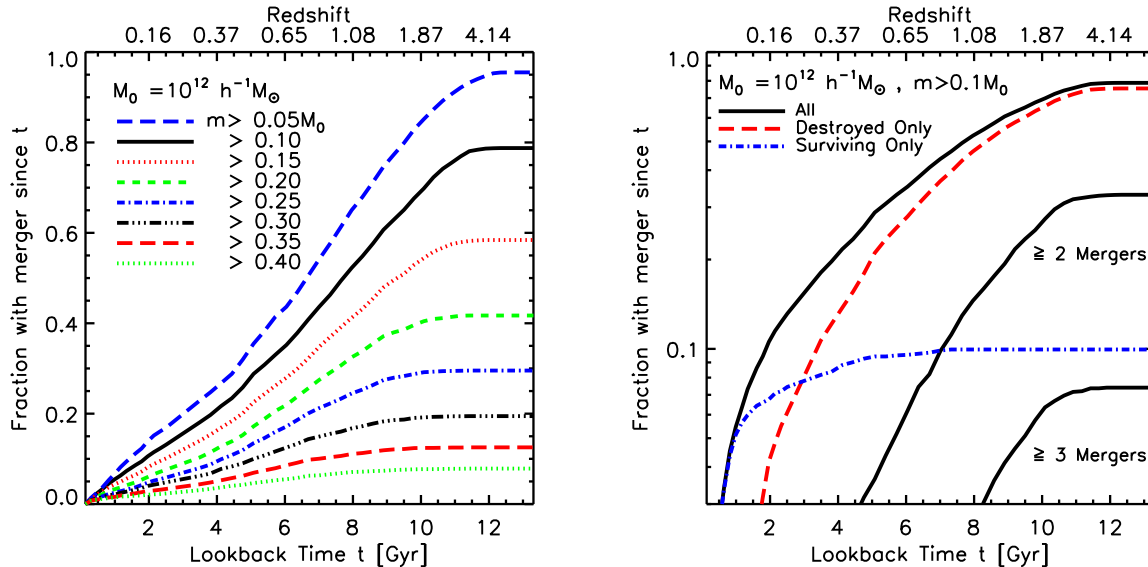


FIG. 5.— *Left:* The fraction of Milky Way-sized halos, $M_0 \simeq 10^{12} h^{-1} M_\odot$, that have experienced at least one merger larger than a given mass threshold, m , since look-back time t . *Right:* The three solid (black) lines show the fraction of $M_0 \simeq 10^{12} h^{-1} M_\odot$ halos that have experienced at least one, two, or three mergers larger than $m = 0.1 M_0$ in a lookback time t . The upper solid line is the same as the solid line in the left panel. The dashed (red) line include only mergers that are “destroyed” before $z = 0$ (*i.e.* lose $> 80\%$ of their mass by $z = 0$). Conversely, the dot-dashed (blue) line shows the fraction of halos with at least one merger that “survives” as a subhalo as a function of lookback time to the surviving halo’s merger. Large accretions of $m > 0.1 M_0$ typically do not survive for more than ~ 3 Gyr after accretion.

tities predicted from Extended Press Schechter (EPS Lacey & Cole 1993) Monte-Carlo merger trees. Each of these lines is based on 5000 trees generated using the Somerville & Kolatt (1999) algorithm.

In broad terms, the mass spectrum of accreted objects agrees fairly well with the EPS expectations, especially considering the relative ambiguity associated with defining halo masses in simulations (e.g. Cohn & White 2007; Diemand et al. 2007; Cuesta et al. 2007). However, it is worth discussing the similarities and differences in some detail. It is a well-known expectation from EPS that the total mass accreted into a halo of mass M_0 is dominated by objects of mass $m \sim 0.1 M_0$ (Lacey & Cole 1993; Zentner & Bullock 2003; Purcell et al. 2007; Zentner 2007). Our simulations reveal that indeed $m \simeq (0.03 - 0.3) M_0$ objects are the most important contributors to the final halo mass.

EPS trees predict self-similar mass fractions across all halo masses. Our more massive halos, however, show a slight tendency to have more of their mass accreted in collapsed objects, across all scaled masses m/M_0 . As discussed in association with Equation 3 above, the overall normalization of the mass spectrum is slightly higher for our more massive halos. For example, the mass accreted in objects larger than $m = 0.01 M_0$ is $\sim 45\%$ for $M_0 = 10^{12}$ halos and $\sim 50\%$ for $M_0 = 10^{13}$ halos. Both of these fractions are low compared to the $\sim 65\%$ expected from the semi-analytic EPS merger trees.

It is interesting to estimate the *total* mass fraction accreted in collapsed objects ($m > 0$) by extrapolating the $n(m)$ fit given in Equation 3 to $m \rightarrow 0$. We find

$$f(> 0) = \int_0^{0.5 M_0} \frac{df}{dm} dm$$

$$= \int_0^{0.5} A x^{1-\alpha} (0.5 - x)^\beta dx \quad (4)$$

$$\simeq 0.24 A.$$

In the second step, β and α are the shape parameters in Equation 3. In the last step we have used our best fit parameters $\alpha = 0.61$ and $\beta = 2.3$. Using Equation 2 for $A(M_0)$, we find that the total accreted mass fraction (in virialized halos) increases from $f \simeq 0.50$ to 0.70 as M_0 varies from $10^{11.5}$ to $10^{13} h^{-1} M_\odot$. This suggests that a significant fraction ($\sim 30 - 50\%$) of dark halo mass is accreted in the form of “diffuse”, unvirialized material, and that smaller halos have a higher fraction of their mass accreted in this diffuse form. Of course, our conclusion on “diffuse” accretion may be due, at least in part, to difficulties in precisely defining halo masses—and, in particular, in defining halo masses in dense environments where mergers are occurring rapidly. It is also possible that the accreted mass function steepens below our resolution limit, resulting in a lower diffuse fraction than we expect from our extrapolation, but there is no clear physical reason to expect such a steepening.

3.2. Merger Statistics

Understanding how galaxy mergers can affect galaxy transformations and morphological fractions necessarily requires an understanding of halo merger statistics. Of specific interest is the overall fraction of halos that have had mergers within a given look back time.

The left panel of Figure 5 shows the fraction of Milky Way-sized halos ($M_0 \sim 10^{12} h^{-1} M_\odot$) that have experienced *at least one* “large” merger within the last t Gyr. The different line types correspond to different absolute mass cuts on the accreted halo, from $m > 0.05 M_0$ to $m > 0.4 M_0$. The tendency for lines to flatten at large

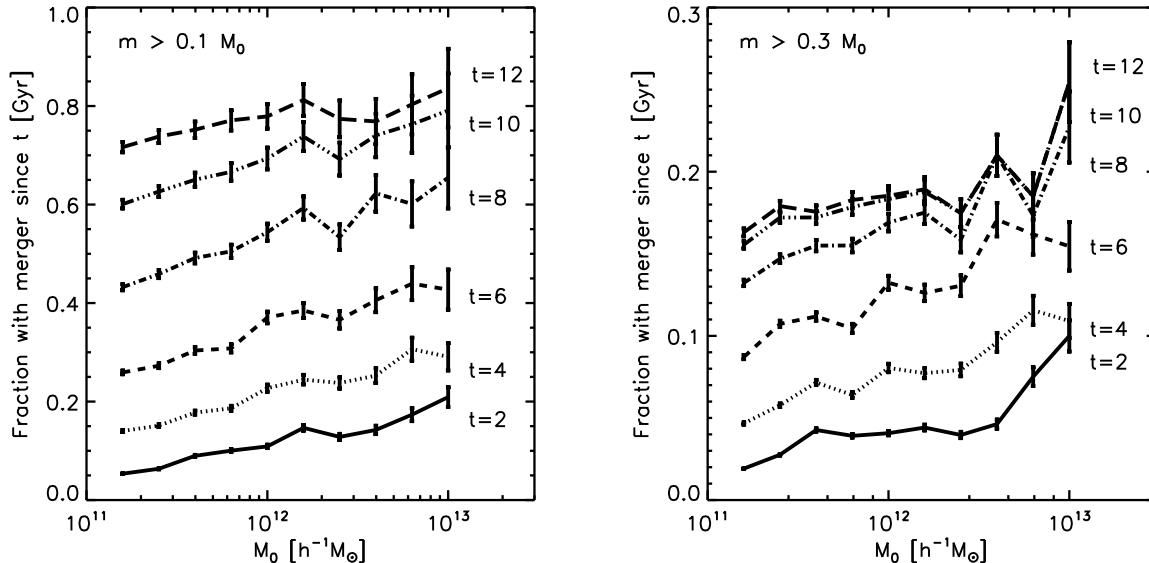


FIG. 6.— The fraction of halos of mass M_0 at $z = 0$ that have experienced a merger with an object more massive than $0.1M_0$ (left) and $0.3M_0$ (right) in the last t Gyr. Error bars are Poissonian based on the number of halos used in each mass bin. Note the fairly weak mass dependence.

lookback times is a physical effect and *is not an artifact of limited resolution*. Specifically, the lines flatten at high z because the halo main progenitor masses, M_z , become smaller than the mass threshold on m (see Figure 2). We find that while less than $\sim 10\%$ of Milky Way-sized halos have *ever* experienced a merger with an object large enough to host a sizeable disk galaxy, ($m > 0.4 M_0 \simeq 4 \times 10^{11} h^{-1} M_\odot$), an overwhelming majority ($\sim 95\%$) have accreted an object more massive than the Milky Way’s disk ($m > 0.05 M_0 \simeq 5 \times 10^{10} h^{-1} M_\odot$). Approximately 70% of halos have accreted an object larger than $m \simeq 10^{11} h^{-1} M_\odot$ in the last 10 Gyr.

While the left panel of Figure 5 illustrates the fraction of halos with at least one merger in a given time, the right panel of Figure 5 provides statistics for multiple mergers. We again focus on $M_0 \sim 10^{12} h^{-1} M_\odot$ halos, but restrict our statistics to accretions with $m > 0.1 M_0 \simeq 10^{11} h^{-1} M_\odot$. The upper solid (black) line shows the fraction of halos with at least one accretion event within the last t Gyr. This reproduces the solid (black) line in the left-hand panel, but now the vertical scale is logarithmic. The middle and lower solid (black) lines in the right panel show the fraction of halos with at least two and at least three mergers larger than $0.1 M_0$ in the past t Gyr, respectively. Roughly $\sim 30\%$ of Milky Way-sized halos have experienced at least two accretion events larger than $\sim 10^{11} h^{-1} M_\odot$. Multiple events of this kind could be important in forming elliptical galaxies (Hernquist 1993; Boylan-Kolchin et al. 2005; Robertson et al. 2006a; Naab et al. 2006).

As discussed above, our merger events are defined at the time when the accreted halo first cross within the virial radius of the main progenitor. This definition allows us to focus on a robust statistic that is less likely to be affected by baryonic components. In §4, we speculate on the implications of these results for disk stability. In this context, one may be concerned that some fraction

of our identified “mergers” will never interact with the central disk region, but instead remain bound as surviving halo substructure. We expect this effect to be most important for smaller accretions, as larger merger events will decay very quickly.

The dashed (red) line in Figure 5 shows a statistic that is analogous to the upper black line — the fraction of halos that have had at least one merger in the last t Gyr — except we have now restricted the analysis to include only objects that are “destroyed” before $z = 0$. We define an object to be “destroyed” if it loses more than 80% of the mass it had at accretion because of interactions with the central halo potential. (Our results are unchanged if we use 70 – 90% thresholds for mass loss). Likewise, the dot-dashed (blue) line shows the same statistic restricted to “surviving” objects. Only $\sim 10\%$ of Milky Way-sized halos have surviving massive substructures at $z = 0$ that are remnants of $m \simeq 10^{11} h^{-1} M_\odot$ accretion events. These survivors were typically accreted within the last ~ 3 Gyr.

We conclude that large accretions that happened more than ~ 3 Gyr ago would have had significant interactions with the central disk regions of the main progenitor. Indeed, this must be the case if the Milky Way is “typical”. The most massive Milky Way satellite, the LMC, was likely accreted with a mass no larger than $m \sim 4 \times 10^{10} h^{-1} M_\odot$ (van der Marel et al. 2002; Robertson et al. 2005). According to Figure 3, we expect that the Milky Way has accreted at least ~ 3 objects that are larger than the LMC over its history. The expectation is that most of the larger objects that were accreted have been shredded by the central galaxy potential, and have deposited their stars in the extended stellar halo (Bullock & Johnston 2005). Interestingly, a recent re-analysis of the LMC’s motion suggests that it is indeed on its first passage about the Milky Way (Besla et al. 2007), as we would expect for surviving, massive satel-

lites.

Given that galaxy morphology fractions are observed to change systematically as a function of luminosity or mass scale (e.g. Park et al. 2007), we are also interested in exploring merger fractions as a function of M_0 . The left panel of Figure 6 shows the fraction of halos that have had a merger larger than $m = 0.1 M_0$ within the last $t = 2, 4, \dots, 12$ Gyr, as indicated by the t labels. The right panel shows the same statistic computed for larger $m > 0.3 M_0$ accretion events. The most striking result is that the merger fraction is fairly independent of M_0 . This suggests that halo merger statistics alone cannot explain the tendency for early-type spheroidal galaxies to reside in more massive halos. Baryon physics must instead play the primary role in setting this trend. (The right-panel in Figure 6 does show evidence that halos larger than $M_0 \sim 3 \times 10^{12} h^{-1} M_\odot$ have a higher fraction of recent ($t \lesssim 2$ Gyr) large ($m > 0.3 M_0$) events, but the overall merger fraction is small ($\lesssim 10\%$), even for group-sized halos with $M_0 \simeq 10^{13} h^{-1} M_\odot$.) When counting *instantaneous* merger rates there appears to be a relatively universal merger rate across a wide range of host masses $M_0 \sim 10^{12} - 10^{14}$ (Fakhouri & Ma 2007). Given this uniformity, we speculate that the weak trend we see in Figure 6 may ultimately be a direct result of the trend for more massive halos to form later, as shown in Figure 2.

If a merger occurs early enough, we might expect the main progenitor halo to grow significantly after the merger. The fraction of mass accreted since the last merger is potentially important, as, for example, it could enable the regrowth of a destroyed disk. One could reason that the fraction of halos that experience a large merger and then subsequently fail to accrete a significant amount of mass is the most relevant statistic for evaluating the probability of disk formation. However, we find that in most cases, very little mass is accreted after an event that is large relative to M_0 .

Figure 7 shows the average *fraction* ($\Delta M/M_0$) of a halo’s final mass M_0 that is accreted since the last large merger. Each curve corresponds to a different threshold in m . As in Figure 6, the overall trend with final mass M_0 is very weak. We define the accreted mass by $\Delta M = M_0 - M_m$, where M_m is the mass of the host halo’s main progenitor *after* the most recent large merger. The upper (solid, black) line includes all halos that have had at least one event larger than $m = 0.1 M_0$ and the lowest line (long-dashed, red) includes all halos that have had at least one merger larger than $m = 0.35 M_0$. This shows that the fractional mass accreted since a merger is a decreasing function of m/M_0 . It also shows that the fraction is typically small, with $\Delta M/M_0 \lesssim 30\%$ (10%) for $m \gtrsim 0.1 M_0$ ($0.3 M_0$) mergers. These trends are a consequence of the fact that we are doing this calculation at a fixed M_0 — if a merger m is large compared to M_0 , then there is little room in the mass budget for new material to be accreted after the merger. This implies, for example, that if a disk is destroyed as a result of a large- m/M_0 accretion event, it is unlikely that a new “disk-dominated” system can be regrown from material that is accreted into the host halo after the merger. However, gaseous material involved in the merger may reform a disk (see e.g. Zurek et al. 1988; Robertson et al. 2006a).

4. DISCUSSION

4.1. Milky Way Comparison

The Milky Way has a dark matter halo of mass $M_0 \simeq 10^{12} h^{-1} M_\odot$ (Klypin et al. 2002), and its stellar mass is dominated by a thin disk of mass $\simeq 3.5 \times 10^{10} M_\odot$ (Klypin et al. 2002; Widrow & Dubinski 2005). The thin disk has vertical scale height that is just $\sim 10\%$ of its radial scale length (Siegel et al. 2002; Juric et al. 2005; Newberg et al. 2006), and contains stars as old as ~ 10 Gyr (Nordström et al. 2004). Moreover, stars in the local thick disk are predominantly older than ~ 10 Gyr, and the bulge is old as well. This suggests that there was not significant merger activity in the Milky Way to drive gas towards the bulge or to thicken the disk in the past ~ 10 Gyr (Wyse 2001).

Based on our results, a galaxy like the Milky Way would seem rare in a Λ CDM universe. Roughly 70% of dark matter halos of mass $M_0 \simeq 10^{12} h^{-1} M_\odot$ have experienced a merger with a halo of mass $10^{11} h^{-1} M_\odot$ in the past ~ 10 Gyr. A merger of this size should thicken the existing disk and drive gas into the center of the galaxy to create a bulge (Kazantzidis et al. 2007). If the Milky Way has *not* experienced a merger of this magnitude, that would make our galaxy a rare occurrence ($\lesssim 30\%$ of halos). On the other hand, if the Milky Way *has* experienced such a merger, it is difficult to understand its observed early-type morphology and thin-disk properties.

4.2. Morphological Fractions and Thick Disks

The degree to which the Milky Way halo is typical for its mass is becoming better understood thanks to the advent of large, homogeneous astronomical sky surveys. As mentioned in the introduction, broad-brush categorizations of “late type” vs. “early type” suggest that $\sim 70\%$ of Milky Way-sized halos host late-type galaxies (e.g. Weinmann et al. 2006; van den Bosch et al. 2007; Ilbert et al. 2006; Choi et al. 2007; Park et al. 2007). The degree to which “late-type” is synonymous with “thin disk-dominated” is difficult to quantify with current data sets, but for the sake of this discussion, we will assume that this is the case. Also discussed earlier were the results of Kautsch et al. (2006), who found that $\sim 16\%$ of disk galaxies are bulgeless systems. This suggests that $\sim (0.7)(0.16) \sim 11\%$ of Milky Way-sized halos host pure disk galaxies.

The observed morphological fractions may be compared to the halo merger fractions presented in Figure 5. These results show that an overwhelming majority of Milky Way-sized halos ($\sim 95\%$) experience at least one merger larger than the *current* mass of the Milky Way disk ($\gtrsim 5 \times 10^{10} h^{-1} M_\odot$). Figure 3 shows that a typical $M_0 \simeq 10^{12} h^{-1} M_\odot$ halo has merged with $\sim 2 - 3$ objects of this size over its history. It is possible that mergers of this characteristic mass are responsible for creating thick disk components in most galaxies (Walker et al. 1996; Dalcanton & Bernstein 2002). More detailed simulations will be required to test whether disks are destroyed or overly thickened by the predicted infall of $m \sim 5 \times 10^{10} h^{-1} M_\odot$ objects, and whether these thickening events happen too late to explain thick disks as old as those observed (Dalcanton & Bernstein 2002). Understanding how bulgeless galaxies could exist in halos with

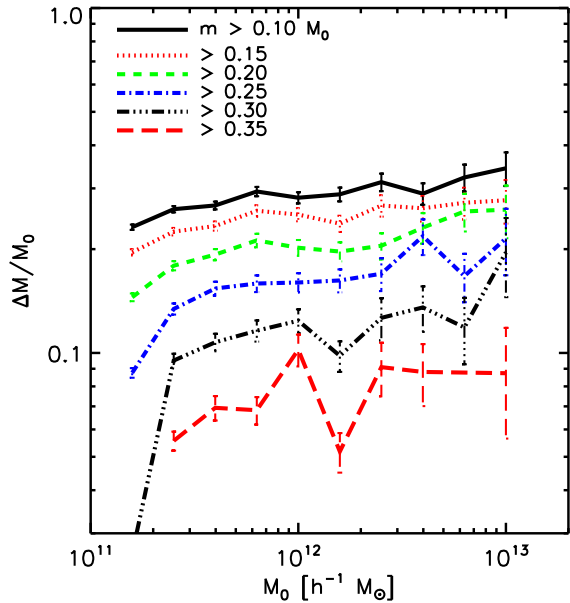


FIG. 7.— The average fractional change in a halo’s main progenitor mass $\Delta M/M_0$ since its last large merger, shown as a function of the halo’s $z = 0$ mass M_0 . Each line includes only halos that have had a merger larger than the m value indicated (*i.e.* only halos that have had a $m > 0.35M_0$ accretion event are included in the lowest line). Error bars shown are Poisson on the number of halos used in the average.

mergers of this kind is a more difficult puzzle.

Perhaps more disturbing for the survival of thin disks are the statistics of more substantial merger events. Figure 5 shows that $m \gtrsim 10^{11}h^{-1}M_\odot$ accretions are quite common in Milky Way-sized halos, with $\sim 70\%$ of $M_0 \simeq 10^{12}h^{-1}M_\odot$ objects experiencing such a merger in the past ~ 10 Gyr. Of course, the impact that these events will have on a central disk will depend on orbital properties, gas fractions, and star formation in the merging systems. Generally, however, a merger with an object ~ 4 times as massive as the Milky Way thin disk would seem problematic for its survival.

We find that a small fraction of a halo’s final mass is typically accreted into the main progenitor subsequent to $m \sim 0.1M_0$ mergers — this suggests that the regrowth of a dominant disk from material accreted *after* such a merger will be difficult (see Figure 7). We conclude that if $\sim 70\%$ of Milky Way-sized halos contain disk-dominated galaxies, and if the adopted Λ CDM cosmology is the correct one, then mergers involving $m \simeq 10^{11}h^{-1}M_\odot$ objects must not result in the destruction of galaxy disks. This is a fairly conservative conclusion because if we naively match the percentages of mergers with an early-type fraction of $\sim 30\%$, then Figure 5 suggest that the critical mass scale for disk survival is significantly larger, $m \gtrsim 2 \times 10^{11}h^{-1}M_\odot$. Specifically, mergers involving objects that are ~ 5 times the current Milky Way disk mass must not (always) destroy disks.

We remind the reader that the lookback times depicted in Figures 5 and 6 correspond specifically to the times when infalling halos first fall within the main progenitor’s virial radius. Our estimates suggest that the corresponding central impacts should occur ~ 3 Gyr later for the mass ratios we consider. Therefore, when we quote

merger fractions to a lookback time of ~ 10 Gyr, this will correspond to an actual impact ~ 7 Gyr ago. Of course, the infalling systems will also lose mass as they fall towards the central galaxy. As we have emphasized, the detailed evolution of merging objects can only be determined with focused simulations, and the outcome of the subsequent mergers will depend on the baryonic components and orbital properties of the systems involved.

Kazantzidis et al. (2007) have performed a focused N-body simulation in order to investigate the morphological response of a thin, Milky Way type stellar disk galaxy to a series of impacts with 6 satellite halos⁷ of mass $m \simeq (1-2) \times 10^{10}M_\odot$ ($\sim 30-60\%$ of the disk mass). They find that a dominant “thin” stellar disk component survives the bombardment, although its scale-height was seen to increase from 250 pc to ~ 400 pc, and a second ~ 1.5 kpc “thick” component was also created. In addition, a new central bar / bulge component was also generated in these fairly small encounters. While it is encouraging to see that a thin disk can survive some bombardment, mergers with objects ~ 6 times as massive as those considered by Kazantzidis et al. should be very common in Milky Way-sized halos. It remains to be seen how the infall of $m \simeq 10^{11}h^{-1}M_\odot$ objects will affect the morphologies of thin, $\sim 4 \times 10^{10}M_\odot$ stellar disks. Moreover, the merger history considered by Kazantzidis et al. extended to fairly recent events. While there was no explicit star formation prescription in these simulations, one would expect a broad range of stellar ages in the thickened disk stars in this case, instead of a predominantly old population—as seems to be observed in actual galaxies.

4.3. Morphology–Luminosity Trends

Another well-established observational trend is the morphology–luminosity relation (recently, Choi et al. 2007; Park et al. 2007), which, when interpreted in terms of a morphology–halo mass relation, demonstrates that the fraction of late-type galaxies contained within dark matter halos is anti-correlated with the mass of the halo (Weinmann et al. 2006). For large galaxy halos, $M_0 \simeq 10^{13}h^{-1}M_\odot$, the late-type fraction is just $\sim 30\%$, compared to $\sim 70\%$ for Milky Way-sized systems (Weinmann et al. 2006; van den Bosch et al. 2007; Ilbert et al. 2006; Choi et al. 2007; Park et al. 2007). The result presented in Figure 6 is perhaps surprising in light of this fact. Specifically, merger histories of galaxy halos are almost self-similar in M_0 when the infalling mass m is selected to be a fixed fraction of M_0 . For example, $\sim 18\%$ (70%) of $M_0 \simeq 10^{12}h^{-1}M_\odot$ halos have experienced an $m > 0.3M_0$ ($0.1M_0$) merger event in the last 10 Gyr. This fraction grows only marginally to $\sim 25\%$ (80%) for $M_0 \simeq 10^{13}h^{-1}M_\odot$ halos. The implication is that dark matter halo merger histories alone cannot explain the observed correlation between early-type fraction and halo mass. Specifically, baryon physics must play the primary role in setting the observed trend between galaxy morphology and halo mass.

⁷ We note that their 6 accretions were chosen from a high-resolution N-body simulation, and that this number of events is fairly typical of what we find based on ~ 2500 Milky Way-sized halos in Figure 4. However, it is also typical of a Milky Way-size halo to experience 1–2 mergers more massive than any of these accretions.

4.4. Successive Minor Mergers

Recently, Bournaud et al. (2007) have used focused simulations to investigate the response of a very massive $\sim 2 \times 10^{11} M_\odot$ disk-dominated galaxy within a $\sim 10^{12} M_\odot$ halo to mergers with total mass *ratios* ranging from $m/M_z = 0.02$ to 1.0. Broadly speaking, they find that $m/M_z = 0.1$ merger ratio events can transform their disk galaxy to an S0, and that $m/M_z = 0.3$ ratio events produce ellipticals. It is unclear how these ratios would change for a smaller primary disk mass, considering that their disk mass is extremely massive for a halo of this size. In comparison, $\sim 95\%$ of our Milky Way-sized halos experience an event with a merger ratio of $m/M_z > 0.1$ (corresponding to $m \gtrsim 0.05 M_0$, see Appendix) in the last 10 Gyr. Similarly, $\sim 60\%$ of our halos experience $m/M_z > 0.3$ events (See Figure 8). We note that the results of this type of simulation will be sensitive to the gas fractions and ISM model of the interacting galaxies (Robertson et al. 2006a).

Hayashi & Chiba (2006) have also investigated the response of a galactic disk to a succession of minor mergers of CDM subhalos. They find that subhalos more massive than 15% of the disk mass must not merge into the thin disk itself, or it will become thicker than the observed disk of the Milky Way. While our merger rates are for subhalos entering the virial radius of the *halo*, not when it penetrates the disk, we expect the fraction of disk mergers involving objects of mass $6 \times 10^9 M_{\text{dot}}$ to be quite high. Recall that 95% of halos experience an accretion event larger than $5 \times 10^{10} M_{\text{dot}}$. Even if these halos lose 90% of their mass before disk impact (which seems unlikely) they still meet the Hayashi and Chiba criterion. Note, however, that a detailed thin/thick decomposition may be required in order to fully evaluate this limit (Kazantzidis et al. 2007). A more detailed study of large mergers, including the necessary baryon physics, is required to fully explore this issue.

4.5. Gas-rich Mergers

Many of our results provide qualitative support to the idea that cool gas-fractions play a fundamental role in governing the morphological outcome of large mergers (Robertson et al. 2006a; Brook et al. 2007a,b; Cox et al. 2007), with gas-rich mergers essential to the formation and survival of disk galaxies. While dark halo merger histories are approximately self-similar in M_0 , gas fractions are known to decrease systematically with halo mass (at least at $z = 0$, see e.g. Geha et al. 2006; Kaufmann et al. 2007b, and references therein). This implies that gas-rich mergers should be more common in small halos than in large halos. If gas-rich mergers do allow for the formation or survival of disk galaxies, then the gas-fraction-mass trend may provide an important ingredient in explaining the observed morphology-mass trend. Specifically, small halos should experience more gas-rich mergers, while large halos should experience more gas-poor mergers. However, stars resulting from a gas-rich merger will be younger than the lookback time of the merger, suggesting that mergers of this type only serve as an adequate explanation for early mergers. Also, these gas-rich mergers would require sufficient angular momentum to keep the resulting disk from being too centrally concentrated.

4.6. Comparison to Previous Work

Semi-analytic models (e.g. Diaferio et al. 2001; Okamoto & Nagashima 2001) and models based on cosmological SPH simulations (Maller et al. 2006) have demonstrated that many of the observed trends between galaxy morphology, density, and luminosity can be explained in Λ CDM-based models. However, these results rely on the ability to *choose* a characteristic galaxy mass ratio for morphological transformation r_{char} (usually $r_{\text{char}} \sim 0.3$). The assumption is that that galaxy-galaxy mergers with $m_{\text{gal}}/M_{\text{gal}} \lesssim r_{\text{char}}$ allow a disk to remain intact, while all larger mergers produce spheroids. In a recent investigation, Koda et al. (2007) have explored a two-parameter model, where stellar spheroid formation depends on both m/M_z and the absolute halo mass, M_z . Host halos with masses smaller than a critical M_z are assumed to have very low baryon content in this picture. Using the PINOCCHIO density-field algorithm (Monaco et al. 2002) to generate halo merger statistics, Koda et al. (2007) find that the fraction of disk-dominated galaxies can be explained if the only events that lead to central spheroid formation have $m/M_z > 0.3$ and $M_z \gtrsim 4 \times 10^{10} h^{-1} M_\odot$.

The goal of this work has not been to find a ratio that can explain morphological fractions. Rather, our aim has been to emphasize the relatively large number of more minor mergers that could potentially be ruinous to disk survival. As discussed in the Appendix, events with $m \simeq 0.1 M_0$ in galaxy halos typically have $m/M_z \simeq 0.2$ at the time of accretion. These $\sim 10^{11} h^{-1} M_\odot$ mergers would produce no morphological response in the primary disk under many standard treatments (e.g. Maller et al. 2006; Koda et al. 2007). For the sake of comparison, Figure 8 in the Appendix shows galaxy halo merger statistics for fixed m/M_z cuts. Our results are in good agreement with those derived by Koda et al. (2007; Figure 4) using the PINOCCHIO algorithm, and with those quoted by Wyse (2006) for an analysis made by L. Hebb using the GIF simulations.

Finally, we mention that Cole et al. (2007) have used the large Millennium Simulation to investigate the progenitor mass functions of halos. In qualitative agreement with our findings, Cole et al. (2007) find that the fraction of mass coming from halo progenitors is lower than expected from standard EPS treatments. Their approach was somewhat different than ours, as they focused on the full progenitor mass function, as opposed to the mass function of objects that merged into the main progenitor as we have here. They estimate that $\sim 14\%$ of a halo's progenitors are not accounted for in collapsed objects at any redshift. This may be compared to our estimate of $\sim 30 - 50\%$ for the fraction of mass not directly accreted in the form of virialized objects for $M_0 = 10^{13}$ to $10^{12} h^{-1} M_\odot$ halos. The differences between our numbers and theirs may come from the fact that we have actually measured slightly different quantities. We also used different halo-finding algorithms and halo mass definitions, and utilized different formulations to extrapolate the simulation results to unresolved masses (a peak heights formulation in their case, and a direct mass function formulation in our case). A more thorough investigation of the differences associated with halo-finding algorithms and mass definitions is reserved for a future paper. For the

purposes of this work, it is useful to point out that while a direct comparison is difficult to make at this time, if anything, our results on overall merger counts seem *low* compared to the results given Cole et al. (2007).

5. CONCLUSION

We have used a high-resolution Λ CDM N -body simulation to investigate the merger histories of $\sim 17,000$ galaxy dark matter halos with masses $M_0 = 10^{11-13}h^{-1}M_\odot$ at $z = 0$. Mergers with objects as small as $m = 10^{10}h^{-1}M_\odot$ were tracked. The principle goal has been to present the raw statistics necessary for tackling the issue of thin disk survival in Λ CDM and for providing a cosmological context for more focused simulations aimed at understanding the role of mergers for processes like morphological transformation, star formation triggering, and AGN fueling.

Our main results may be summarized as follows:

1. Mass accretion into halos of mass M_0 at $z = 0$ is dominated by mergers with objects of mass $m \simeq (0.03 - 0.3)M_0$ (Figure 4). Typically, $\sim 1 - 4$ mergers of this size occur over a halo’s history (Figure 3). Because these mergers tend to occur when the main progenitor’s mass, M_z , was somewhat smaller than M_0 , these dominant events have fairly large *merger ratios*, $m/M_z \simeq 0.1 - 0.6$ (see Appendix).
2. The mass accretion function, $n(m)$, of mergers larger than m accreted over a halo’s history is well-described, on average, by a simple analytic form, $n(x \equiv m/M_0) = Ax^{-\alpha}(0.5 - x)^\beta$, with $\alpha = 0.61$ and $\beta = 2.3$. The normalization increases as a function of the halo’s mass at $z = 0$, M_0 , as $A \simeq 0.47 \log_{10}(M_0) - 3.2$. By extrapolating this fit, we find that the total mass fraction accreted in objects of any mass ($m > 0$) does not asymptote to 1.0, but rather increases with M_0 from $\sim 50\%$ in $M_0 = 10^{11.5}h^{-1}M_\odot$ halos to $\sim 70\%$ in $M_0 = 10^{13}h^{-1}M_\odot$ halos. This suggests that a non-zero fraction of a halos mass may be accreted as truly “diffuse” material.
3. An overwhelming majority (95%) of Milky Way-sized halos with $M_0 \simeq 10^{12}h^{-1}M_\odot$ have accreted an object larger than the Milky Way’s disk ($m \gtrsim 5 \times 10^{10}h^{-1}M_\odot$) in the last 10 Gyr. Approximately 70% have had accretions with $m > 10^{11}h^{-1}M_\odot$ objects over the same period, and 40% have had $m > 2 \times 10^{11}h^{-1}M_\odot$ events (Figure 5).
4. Halo merger histories are approximately self-similar in m/M_0 for halos with masses in the range $M_0 = 10^{11} - 10^{13}h^{-1}M_\odot$ (Figure 6). This suggests that the empirical trend for late-type galaxies to be more common in smaller halos is not governed by differences in merger histories, but rather is associated with baryon physics.
5. Typically, a small fraction, $\sim 20 - 30\%$, of a halo’s final mass M_0 is accreted *after* the most recent large merger with $m > (0.1 - 0.2)M_0$ objects (Figure 7). This suggests that the “regrowth” of a disk from newly accreted material after a large merger is unlikely. Note that this does not rule out the pos-

sibility that a disk reforms from gaseous material involved in the merger itself.

The relatively high fraction of halos with large $m \sim 0.1M_0$ merger events raises concerns about the survival of thin disk galaxies within the current paradigm for galaxy formation in a Λ CDM universe. If we naively match percentages using Figure 5, we find that in order to achieve a $\sim 70\%$ disk-dominated fraction in $M_0 = 10^{12}h^{-1}M_\odot$ halos, then $m \simeq 0.2M_0 \simeq 2 \times 10^{11}h^{-1}M_\odot \simeq 3 \times 10^{11}M_\odot$ objects must not (always) destroy disks. Furthermore, since stars in the local thick disk and bulge are predominantly older than ~ 10 Gyr, this suggests that these mergers in the past ~ 10 Gyr must not drive gas towards the bulge or significantly thicken the disk. Note that the total mass in such an accreted object is ~ 10 times that of the Milky Way disk itself. Moreover halos typically do not accrete a significant fraction of their final mass after these mergers ($\sim 20\%$ on average). Finally, as noted in the Appendix, $m \sim 0.2M_0$ events typically have merger *ratios* of $m/M_z \simeq 0.4$ at the time of the merger. These numbers do not seem encouraging for disk survival, and may point to a serious problem with our current understanding of galaxy formation in a Λ CDM universe.

Our basic conclusion is unlikely to be sensitive to uncertain cosmological parameters. Note that the simulations considered here have a fairly high $\sigma_8 = 0.9$. At a fixed Ω_m , a lower σ_8 will systematically produce slightly *more* recent merger events (e.g. Zentner & Bullock 2003). However, given that the merger fractions measured using m/M_0 are approximately self-similar in M_0 (and therefore in M_0/M_*), we expect that the overall merger fractions will be fairly insensitive to power-spectrum normalization.

As discussed in the introduction, a complete investigation into the issue of disk survival will require an understanding of the orbital evolution of objects once they have fallen within the main progenitor halo’s virial radius and on the subsequent impact of interacting galaxies. Both of these outcomes will depend sensitively on the baryonic components in the main halo and in the smaller merging object. For this reason, the present work has focused on *halo mergers*, defined to occur when an infalling halo first crosses within the virial radius of the main progenitor halo. The merger statistics presented here are relatively devoid of uncertainties and can be used as a starting point for direct simulations of galaxy-galaxy encounters. Simulations of this kind will be essential to fully address the broader implications of these frequent, large mergers, which seem to pose a serious challenge to disk survival.

The simulation used in this paper was run on the Columbia machine at NASA Ames. We would like to thank Anatoly Klypin for running the simulation and making it available to us. We are also indebted to Brandon Allgood for providing the merger trees. We thank Chris Brook, T. J. Cox, Fabio Governato, Christian Maulbetsch, Brant Robertson, Matias Steinmetz, Jerry Sellwood, and Rosemary Wyse for helpful comments on an earlier draft, and Onsi Fakhouri and Chung-Pei Ma for useful discussions about halo merger rates. We thank the anonymous referee for several insightful suggestions that helped to improve the quality and clarity of the paper.

JSB, RHW, and AHM thank Rarija Mechslock for inspiration at an early phase of this project. JSB and KRS are supported by NSF grant AST 05-07916. RHW was supported in part by the U.S. Department of Energy under contract number DE-AC02-76SF00515 and by a Terman

Fellowship from Stanford University. ARZ is funded by the University of Pittsburgh. AHM acknowledges partial support from a CUNY GRTI-ROUND 9 grant and from an ROA supplement to NSF grant AST 05-07916.

REFERENCES

- Abadi, M. G., Navarro, J. F., Steinmetz, M., & Eke, V. R. 2003, *ApJ*, 591, 499
- Allgood, B., Flores, R. A., Primack, J. R., Kravtsov, A. V., Wechsler, R. H., Faltenbacher, A., & Bullock, J. S. 2006, *MNRAS*, 367, 1781
- Barnes, J. E. 1988, *ApJ*, 331, 699
- Barton, E. J., Arnold, J. A., Zentner, A. R., Bullock, J. S., & Wechsler, R. H. 2007, arXiv:0708.2912 [astro-ph]
- Bell, E. F., Zucker, D. B., Belokurov, V., Sharma, S., Johnston, K. V., Bullock, J. S., Hogg, D. W., Jahnke, K., de Jong, J. T. A., Beers, T. C., Evans, N. W., Grebel, E. K., Ivezić, Z., Koposov, S. E., Rix, H.-W., Schneider, D. P., Steinmetz, M., & Zolotov, A. 2007, arXiv:0706.0004 [astro-ph]
- Besla, G., Kallivayalil, N., Hernquist, L., Robertson, B., Cox, T. J., van der Marel, R. P., & Alcock, C. 2007, arXiv:0703196 [astro-ph]
- Blumenthal, G. R., Faber, S. M., Primack, J. R., & Rees, M. J. 1984, *Nature*, 311, 517
- Bournaud, F., Jog, C. J., & Combes, F. 2007, ArXiv e-prints, 709
- Boylan-Kolchin, M., Ma, C.-P., & Quataert, E. 2005, *MNRAS*, 362, 184
- . 2007, arXiv:0707.2960 [astro-ph]
- Brook, C., Richard, S., Kawata, D., Martel, H., & Gibson, B. K. 2007a, *ApJ*, 658, 60
- Brook, C. B., Kawata, D., Gibson, B. K., & Freeman, K. C. 2004, *ApJ*, 612, 894
- Brook, C. B., Veilleux, V., Kawata, D., Martel, H., & Gibson, B. K. Gas Rich Mergers in Disk Formation (Island Universes - Structure and Evolution of Disk Galaxies), 551+
- Bryan, G. L. & Norman, M. L. 1998, *ApJ*, 495, 80
- Bullock, J. S. & Johnston, K. V. 2005, *ApJ*, 635, 931
- Bullock, J. S., Kravtsov, A. V., & Weinberg, D. H. 2001, *ApJ*, 548, 33
- Carollo, C. M., Scarlata, C., Stiavelli, M., Wyse, R. F. G., & Mayer, L. 2007, *ApJ*, 658, 960
- Choi, Y.-Y., Park, C., & Vogeley, M. S. 2007, *ApJ*, 658, 884
- Cohn, J. D. & White, M. 2007, arXiv:0706.0208 [astro-ph]
- Cole, S., Helly, J., Frenk, C. S., & Parkinson, H. 2007, arXiv:0708.1376 [astro-ph]
- . 2008, *MNRAS*, 383, 546
- Cox, T. J., Dutta, S. N., Di Matteo, T., Hernquist, L., Hopkins, P. F., Robertson, B., & Springel, V. 2006a, *ApJ*, 650, 791
- . 2006b, *ApJ*, 650, 791
- Cox, T. J., Jonsson, P., Somerville, R. S., Primack, J. R., & Dekel, A. 2007, arXiv:0709.3511 [astro-ph]
- Cuesta, A. J., Prada, F., Klypin, A., & Moles, M. 2007, arXiv:0710.5520 [astro-ph]
- Dalcanton, J. J. & Bernstein, R. A. 2002, *AJ*, 124, 1328
- Dalcanton, J. J., Seth, A., & Yoachim, P. 2005, arXiv:astro-ph/0509700
- Davis, M., Efstathiou, G., Frenk, C. S., & White, S. D. M. 1985, *ApJ*, 292, 371
- Diaferio, A., Kauffmann, G., Balogh, M. L., White, S. D. M., Schade, D., & Ellingson, E. 2001, *MNRAS*, 323, 999
- Diemand, J., Kuhlen, M., & Madau, P. 2007, *ApJ*, 667, 859
- Fakhouri, O. & Ma, C.-P. 2007, arXiv:0710.4567 [astro-ph]
- Geha, M., Blanton, M. R., Masjedi, M., & West, A. A. 2006, *ApJ*, 653, 240
- Governato, F., Willman, B., Mayer, L., Brooks, A., Stinson, G., Valenzuela, O., Wadsley, J., & Quinn, T. 2007, *MNRAS*, 374, 1479
- Hayashi, H. & Chiba, M. 2006, *PASJ*, 58, 835
- Helmi, A. & White, S. D. M. 1999, *MNRAS*, 307, 495
- Hernquist, L. 1993, *ApJ*, 409, 548
- Ilbert et al. 2006, *A&A*, 453, 809
- Jesseit, R., Naab, T., Peletier, R. F., & Burkert, A. 2007, *MNRAS*, 376, 997
- Johnston, K. V., Hernquist, L., & Bolte, M. 1996, *ApJ*, 465, 278
- Juric, M., Ivezić, Z., Brooks, A., Lupton, R. H., Schlegel, D., Finkbeiner, D., Padmanabhan, N., Bond, N., Rockosi, C. M., Knapp, G. R., Gunn, J. E., Sumi, T., Schneider, D., Barentine, J. C., Brewington, H. J., Brinkmann, J., Fukugita, M., Harvanek, M., Kleinman, S. J., Krzesinski, J., Long, D., Neilsen, E. H., Jr., Nitta, A., Snedden, S. A., & York, D. G. 2005, arXiv:0510520 [astro-ph]
- Kaufmann, T., Mayer, L., Wadsley, J., Stadel, J., & Moore, B. 2007a, *MNRAS*, 53
- Kaufmann, T., Wheeler, C., & Bullock, J. S. 2007b, arXiv:0706.0210 [astro-ph], 706
- Kautsch, S. J., Grebel, E. K., Barazza, F. D., & Gallagher, III, J. S. 2006, *A&A*, 445, 765
- Kazantzidis, S., Bullock, J. S., Zentner, A. R., Kravtsov, A. V., & Moustakas, L. A. 2007, arXiv:0708.1949 [astro-ph]
- Khochfar, S. & Burkert, A. 2005, *MNRAS*, 359, 1379
- Klypin, A., Gottlöber, S., Kravtsov, A. V., & Khokhlov, A. M. 1999, *ApJ*, 516, 530
- Klypin, A. & Holtzman, J. 1997, ArXiv Astrophysics e-prints
- Klypin, A., Zhao, H., & Somerville, R. S. 2002, *ApJ*, 573, 597
- Koda, J., Milosavljevic, M., & Shapiro, P. R. 2007, arXiv:0711.3014 [astro-ph]
- Kolatt, T. S., Bullock, J. S., Somerville, R. S., Sigad, Y., Jonsson, P., Kravtsov, A. V., Klypin, A. A., Primack, J. R., Faber, S. M., & Dekel, A. 1999, *ApJ*, 523, L109
- Kormendy, J. & Fisher, D. B. 2005, in *Revista Mexicana de Astronomia y Astrofisica Conference Series*, Vol. 23, *Revista Mexicana de Astronomia y Astrofisica Conference Series*, ed. S. Torres-Peimbert & G. MacAlpine, 101–108
- Kormendy, J. & Kennicutt, Jr., R. C. 2004, *ARA&A*, 42, 603
- Kravtsov, A. V., Berlind, A. A., Wechsler, R. H., Klypin, A. A., Gottlöber, S., Allgood, B., & Primack, J. R. 2004, *ApJ*, 609, 35
- Kravtsov, A. V., Klypin, A. A., & Khokhlov, A. M. 1997, *ApJS*, 111, 73
- Lacey, C. & Cole, S. 1993, *MNRAS*, 262, 627
- Li, Y., Mo, H. J., van den Bosch, F. C., & Lin, W. P. 2007, *MNRAS*, 379, 689
- Maller, A. H., Katz, N., Kereš, D., Davé, R., & Weinberg, D. H. 2006, *ApJ*, 647, 763
- Mihos, J. C. & Hernquist, L. 1996, *ApJ*, 464, 641
- Monaco, P., Theuns, T., & Taffoni, G. 2002, *MNRAS*, 331, 587
- Naab, T. & Burkert, A. 2003, *ApJ*, 597, 893
- Naab, T., Khochfar, S., & Burkert, A. 2006, *ApJ*, 636, L81
- Navarro, J. F. & Steinmetz, M. 2000, *ApJ*, 538, 477
- Neistein, E. & Dekel, A. 2008, arXiv:0802.0198 [astro-ph], 802
- Newberg, H. J., Mayeur, P. A., Yanny, B., & the SEGUE collaboration. 2006, *Memorie della Societa Astronomica Italiana*, 77, 1049
- Nordström, B., Mayor, M., Andersen, J., Holmberg, J., Pont, F., Jørgensen, B. R., Olsen, E. H., Udry, S., & Mowlavi, N. 2004, *A&A*, 418, 989
- Okamoto, T. & Nagashima, M. 2001, *ApJ*, 547, 109
- Park, C., Choi, Y.-Y., Vogeley, M. S., Gott, J. R. I., & Blanton, M. R. 2007, *ApJ*, 658, 898
- Peebles, P. J. E. 1982, *ApJ*, 263, L1
- Purcell, C. W., Bullock, J. S., & Zentner, A. R. 2007, *ApJ*, in press, arXiv:astro-ph/0703004
- Quinn, P. J., Hernquist, L., & Fullagar, D. P. 1993, *ApJ*, 403, 74
- Robertson, B., Bullock, J. S., Cox, T. J., Di Matteo, T., Hernquist, L., Springel, V., & Yoshida, N. 2006a, *ApJ*, 645, 986
- Robertson, B., Bullock, J. S., Font, A. S., Johnston, K. V., & Hernquist, L. 2005, *ApJ*, 632, 872
- Robertson, B., Cox, T. J., Hernquist, L., Franx, M., Hopkins, P. F., Martini, P., & Springel, V. 2006b, *ApJ*, 641, 21
- Robertson, B., Hernquist, L., Cox, T. J., Di Matteo, T., Hopkins, P. F., Martini, P., & Springel, V. 2006c, *ApJ*, 641, 90
- Robertson, B., Yoshida, N., Springel, V., & Hernquist, L. 2004, *ApJ*, 606, 32

Siegel, M. H., Majewski, S. R., Reid, I. N., & Thompson, I. B. 2002, *ApJ*, 578, 151
 Somerville, R. S. & Kolatt, T. S. 1999, *MNRAS*, 305, 1
 Sommer-Larsen, J., Götz, M., & Portinari, L. 2003, *ApJ*, 596, 47
 Tasitsiomi, A., Kravtsov, A. V., Gottlöber, S., & Klypin, A. A. 2004, *ApJ*, 607, 125
 Toomre, A. & Toomre, J. 1972, *ApJ*, 178, 623
 Toth, G. & Ostriker, J. P. 1992, *ApJ*, 389, 5
 van den Bosch, F. C., Yang, X., Mo, H. J., Weinmann, S. M., Macciò, A. V., More, S., Cacciato, M., Skibba, R., & Kang, X. 2007, *MNRAS*, 376, 841
 van der Marel, R. P., Alves, D. R., Hardy, E., & Suntzeff, N. B. 2002, *AJ*, 124, 2639
 Walker, I. R., Mihos, J. C., & Hernquist, L. 1996, *ApJ*, 460, 121
 Wechsler, R. H., Bullock, J. S., Primack, J. R., Kravtsov, A. V., & Dekel, A. 2002, *ApJ*, 568, 52
 Wechsler, R. H., Zentner, A. R., Bullock, J. S., Kravtsov, A. V., & Allgood, B. 2006, *ApJ*, 652, 71
 Weinmann, S. M., van den Bosch, F. C., Yang, X., & Mo, H. J. 2006, *MNRAS*, 366, 2

Widrow, L. M. & Dubinski, J. 2005, *ApJ*, 631, 838
 Woods, D. F., Geller, M. J., & Barton, E. J. 2006, *AJ*, 132, 197
 Wyse, R. F. G. 2001, in *Astronomical Society of the Pacific Conference Series*, Vol. 230, *Galaxy Disks and Disk Galaxies*, ed. J. G. Funes & E. M. Corsini, 71–80
 Wyse, R. F. G. 2006, in *The Local Group as an Astrophysical Laboratory*, ed. M. Livio & T. M. Brown, 33–46
 Younger, J. D., Cox, T. J., Seth, A. C., & Hernquist, L. 2007, arXiv:0707.4481 [astro-ph]
 Zentner, A. R. 2007, *International Journal of Modern Physics D*, 16, 763
 Zentner, A. R., Berlind, A. A., Bullock, J. S., Kravtsov, A. V., & Wechsler, R. H. 2005, *ApJ*, 624, 505
 Zentner, A. R. & Bullock, J. S. 2003, *ApJ*, 598, 49
 Zhao, D. H., Mo, H. J., Jing, Y. P., & Börner, G. 2003, *MNRAS*, 339, 12
 Zurek, W. H., Quinn, P. J., & Salmon, J. K. 1988, *ApJ*, 330, 519

APPENDIX

The bulk of the paper focused on statistics of halo mergers at a fixed absolute mass threshold m on the merging objects. In this section we present statistics for m/M_z — the merger ratio relative to the main progenitor mass M_z at the redshift z prior to accretion. By definition, $M_z \leq M_0$, causing merger statistics to show larger accretions when presented in terms of m/M_z . For example, the merger ratio equivalent to Figure 3 (bottom panel) fits to $f(> x) = Ax^{-\alpha}(1-x)^\beta$ instead of Equation 3 (to better than 10% across mass range $10^{11.5} - 10^{13.5} h^{-1} M_\odot$), with parameters $A(M_0) \simeq 0.05 \log_{10}(M_0) - 2.0$, $\alpha = 0.04$, and $\beta = 2.0$, and M_0 in units of $h^{-1} M_\odot$. The m/M_z equivalent for $n(> x)$ also fits to this equation (to better than 10% in the mass range $10^{12.0} - 10^{13.5} h^{-1} M_\odot$) with parameters $\alpha \simeq 0.4$, $\beta \simeq 2.0$, and $A(M_0) \simeq 2.0 \log_{10}(M_0) - 21.5$. Given that our simulation output has a fixed physical mass resolution, $m_{\text{res}} = 10^{10} h^{-1} M_\odot$, and that halo main progenitor masses, M_z , vary as a function redshift, the completeness in m/M_z will, in principle, vary from halo to halo as a function of each particular mass accretion track and lookback time. We have accounted for this variable completeness limit in an average sense in what follows.

The *left* panel of Figure 8 shows the fraction of $M_0 = 10^{12} h^{-1} M_\odot$ halos that have experienced *at least one* merger larger than a given threshold ratio ($r_t = 0.1, 0.2, \dots, 0.9$) in m/M_z in the last t Gyr. This result may be compared to Figure 5, which shows the analogous fraction computed using fixed absolute m cuts relative to M_0 . In order to provide results that are robust to our completeness limit in m , for each threshold cut, r_t , the lines are truncated at the lookback time when the *average* $M_0 = 10^{12} h^{-1} M_\odot$ halo’s mass falls below $M_z = m_{\text{res}}/r_t$. We see that $\sim 50\%$

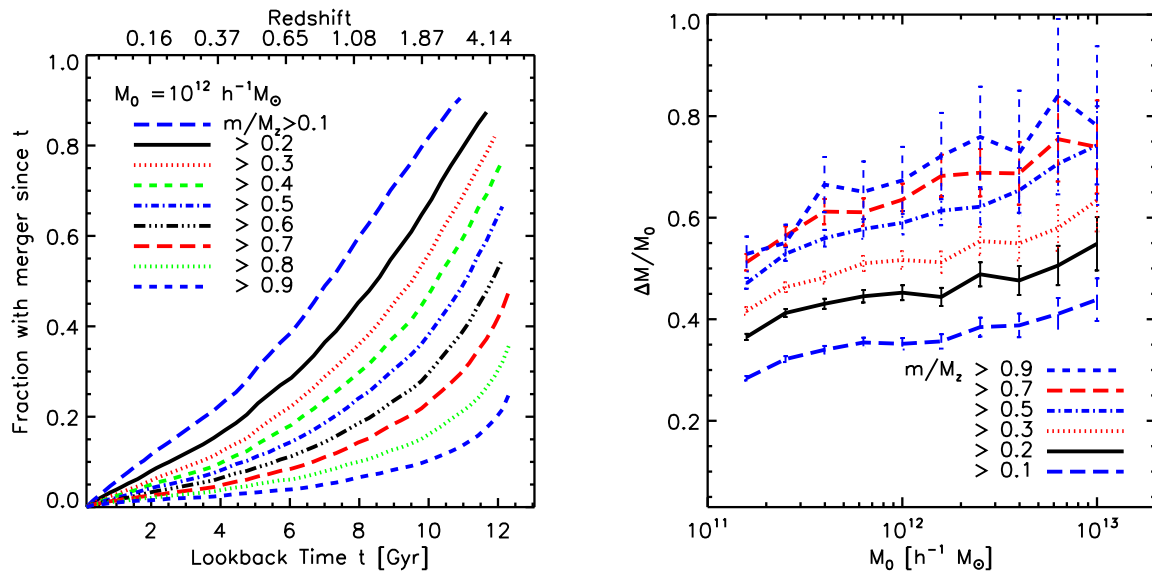


FIG. 8.— *Left*: The fraction of Milky Way-sized halos, $M_0 \simeq 10^{12} h^{-1} M_\odot$, that have experienced at least one merger larger than a given ratio m/M_z since look-back time t , where M_z is the main progenitor mass at the time of accretion. Lines are truncated at epochs where the mass resolution of the simulation limits our ability to resolve a given m/M_z ratio (*i.e.* when M_z gets so small that a quoted m/M_z ratio falls below the resolution with $m > 10^{10} h^{-1} M_\odot$). *Right*: The average change in mass $\Delta M/M_0$ that a halo experiences since its last major merger. Different lines show different “major merger” ratios, m/M_z , where the ratio is defined relative to the main progenitor mass at the time of accretion. Error bars show Poissonian \sqrt{N} errors on the number of host halos averaged.

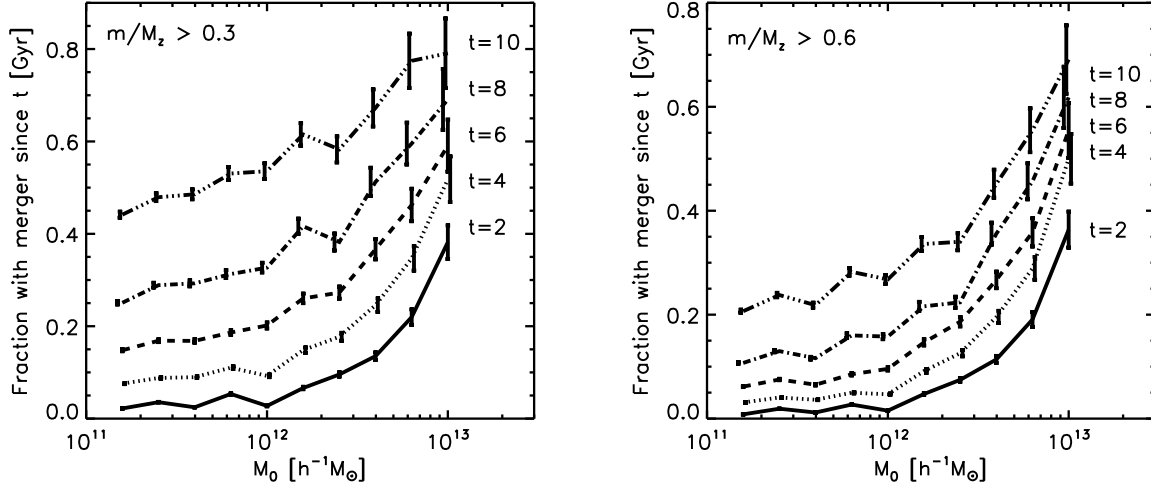


FIG. 9.— *Left:* The fraction of halos of mass M_0 at $z = 0$ that have experienced a merger ratio larger than $m/M_z = 0.3$ in the last t Gyr. The ratio is defined relative to the main progenitor mass at the time prior to accretion M_z . Error bars are Poissonian based on the number of halos used in each mass bin. Note the strong mass trend, in contrast to the results presented in Figure 6, where mergers were defined on a strict mass threshold, rather than merger ratio. *Right:* The fraction of halos of mass M_0 at $z = 0$ that have experienced a merger ratio larger than $m/M_z = 0.6$ in the last t Gyr. The ratio is defined relative to the main progenitor mass at the time prior to accretion M_z . Error bars are Poissonian based on the number of halos used in each mass bin. Note the strong mass trend, in contrast to the results presented in Figure 6, where mergers were defined on a strict mass threshold, rather than merger ratio.

of halos have had a $m/M_z > 0.4$ event in the last ~ 10 Gyr, and that $\sim 10\%$ have experienced nearly equal-mass mergers, $m/M_z > 0.9$, in this time. These results are in good agreement with similar results quoted by Wyse (2006) for an analysis made by L. Hebb using the GIF simulations.

The right panel of Figure 8 shows that, typically, the largest m/M_z events occur *before* most of the final halo mass M_0 is accreted. Specifically we show the fraction of mass $\Delta M/M_0$ accreted since the last major merger. Results for different major merger ratio thresholds are shown as different line types. Each line presents the *average* $\Delta M/M_0$ at fixed M_0 and we only include halos that have actually had a merger of a given ratio (within the last ~ 11 Gyr) in this figure. Among halos that have had nearly equal-mass merger events, $m/M_z \gtrsim 0.9$, the fraction of mass that is accreted since that time is significant, with $\Delta M/M_0 \sim 70\%$ for $M_0 = 10^{12} h^{-1} M_\odot$ halos. If we associate post-merger accretion with the potential “regrowth” of a galactic disk, then, by comparison with Figure 7, high merger-ratio events are less of a concern for disk formation than high m/M_0 ratio events. Unlike most high m/M_z events, mergers that are large relative to M_0 typically have very little ($\lesssim 20\%$) fractional mass accretion after the merger.

The *left panel* of Figure 9 shows the fraction of halos that have had a merger larger than $m/M_z = 0.3$ within the last $t = 2, 4, \dots, 10$ Gyr, as a function of halo mass M_0 . The *right panel* shows the same statistic computed for larger $m/M_z > 0.6$ mergers. Unlike the result shown in Figure 6, there is a fairly significant mass trend, with more massive halos more likely to have experienced a major merger at a fixed lookback time. Note, however, that most of these “major mergers” involve relatively small objects in an absolute sense. Much of this trend is driven by the fact that M_z falls off more rapidly with z for high M_0 halos compared to low M_0 halos.

The previous discussions lead to explore the relationship between an accreted halo’s absolute mass m and the mass-ratio it had when it was accreted, m/M_z . The two panels of Figure 10 illustrate this relationship for objects accreted into $M_0 = 10^{12} h^{-1} M_\odot$ halos. The thick, solid line in the *left panel* shows the median merger ratio, m/M_z , that a halo of mass m/M_0 has when it was accreted. Specifically, we plot m/M_z *given* m/M_0 in this diagram. We see that typically $m/M_z \simeq 2 m/M_0$, as shown by the dashed line in the figure. The dotted lines show the 68 % spread in the distribution of m/M_z given m/M_0 . The opposite relationship is shown in the *right panel* of Figure 10. Here, the thick, solid line shows the median m/M_0 value *given* a merger of mass ratio m/M_z . We see that the majority of high-ratio events involve objects that are small compared to the final halo mass M_0 . Note that this result, and the associated distributions, are complete only to mergers that occur within the past ~ 11 Gyr. If we were able to track main progenitor masses M_z back to arbitrarily early times, we would expect a very larger number of high m/M_z events with small absolute m/M_0 values.

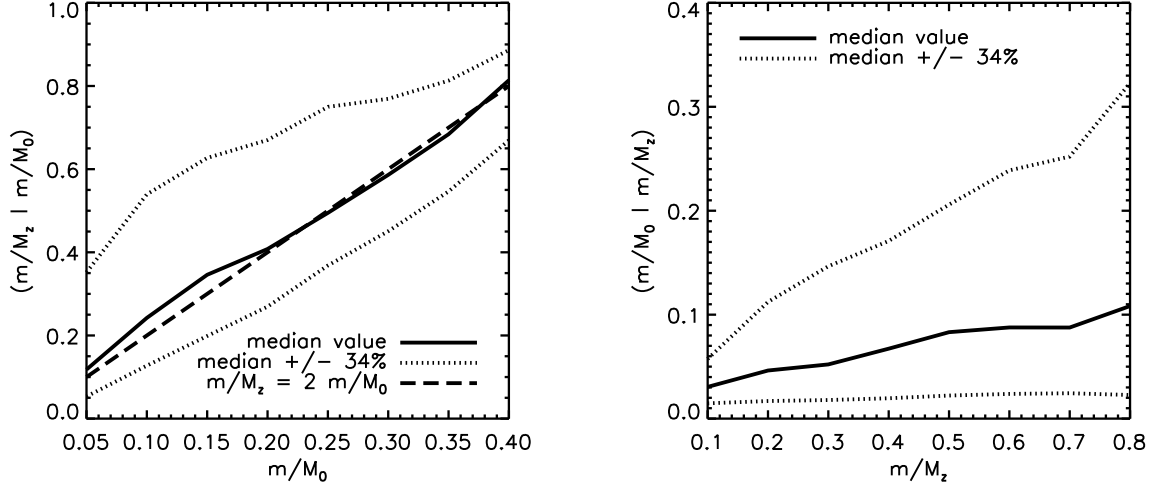


FIG. 10.— *Left:* An illustration of $P(m/M_z|m, M_0)$ — the distribution of merger ratio m/M_z at the time of accretion given a value of m for $M_0 = 10^{12}h^{-1}M_\odot$ halos. We plot m/M_z vs. m/M_0 for clarity. The solid line shows the median and the dotted lines show the 68% spread. *Right:* An illustration of $P(m/M_0|m/M_z)$ — the distribution of merging masses m given a merger ratio m/M_z . We see that the majority of high m/M_z events occur with M_z is small compared to the final halo mass M_0 . Therefore most high-mass ratio mergers are small m mergers in an absolute sense.